TECHNICAL NOTE

Deep SiO_2 etching with Al and AlN masks for MEMS devices

Vladimir Bliznetsov[1], Hua Mao Lin[1], Yue Jia Zhang[1] and David Johnson[2]

[1] Institute of Microelectronics, A*STAR (Agency for Science, Technology and Research),
11 Science Park Road, Singapore Science Park II, Singapore, 117685

[2] SPTS Technologies, Ringland Way, Newport, NP 18 2TA, UK

E-mail: vladimir@ime.a-star.edu.sg

Abstract. Silicon oxide-based materials such as quartz and silica are widely used in Microelectromechanical Systems (MEMS). One way to enhance capability of their deep plasma etching is to increase selectivity by the use of hard masks. Though this approach was studied previously, information on the use of hard masks for etching of silicon-oxide based materials on 200 mm substrates is scarce. We present results of etching process development for amorphous silicon oxide using Al and AlN masks with a view of application of results for etching of silica and quartz. Three gas chemistries (C_4F_8/O_2, CF_4 and SF_6) and their mixtures were compared in an industrial reactive ion etch (RIE) chamber with two plasma sources. It was established that pure SF_6 is the best etchant and AlN is better mask than Al for providing higher selectivity and sidewall angle close to vertical. A range of etching parameters for micromasking-free etching was established and etched structures of up to 4:1 aspect ratio were created in 21μm- thick oxide using the process with etch rate of 0.32-0.36 μm/min and selectivity to AlN mask of (38-49):1.

1. Introduction

In the last decade a few MEMS applications have required deep anisotropic etching of doped and undoped silicon oxide films as well as silicon oxide-based glasses and quartz. Among these groups are quartz resonators, optical MEMS and micro total analysis systems (μTAS) or bio-MEMS. Previously, deep etching of quartz, silica and other glasses was evaluated for substrates with diameter ≤ 150 mm and found application in the prototyping of mentioned devices. Therefore, engineers continued to put efforts into improvement of deep etch of these materials [1-9]. It is known that deep and high aspect ratio etching of glasses is not feasible with standard photoresist masks due to low selectivity and mask profile degradation during prolonged process, therefore, the use of metal or hard masks is preferable.

A few metal masks with different gas mixtures have been investigated so far. In [2] electroplated Cr hard mask was created by wet etching and used for etching of borosilicate glass in RIE chamber with two RF plasma sources (inductively coupled plasma (ICP) and capacitevely coupled plasma (CCP)) using SF_6/Ar chemistry; 32 μm-deep trenches with aspect ratio 2:1 have been achieved. However, limited selectivity SiO_2/Cr of only 35:1 required very thick (3μm) Cr mask, which is an obstacle for using this approach for etching structures with higher aspect ratios. In [3], even thicker, 5 μm Ni mask was created by electroplating with subsequent lift-off and used for etching different glasses with selectivity (23-35):1. Aspect ratio of 2.5 was reported for 100 μm deep structures with sidewall angle 78°. Very thick (300 μm) Ni shadow mask was investigated recently for deep etching of quartz in RIE system, however, the process

displayed micromasking effect which was only partially reduced by adding Ar to SF_6, despite low aspect ratio (<1) [4].

Further increase of aspect ratio requires higher selectivity to mask. In [5, 6] this issue was solved by converting Al mask into Al_2O_3 by using alternating etch–oxidize steps. During oxidation steps, the surface layer of Al was converted into Al_2O_3 that yielded selectivity SiO_2 /Al_2O_3 about 100:1. Due to high selectivity to mask, 5μm -thick SiO_2 waveguides were etched with profile close to vertical using initial Al mask of only 100 nm. However, ratio of oxidation time to etch time was about 1:1, hence, the process duration increased twice and throughput suffered considerably.

Other researchers also reported on high selectivity possible with Al_2O_3 and AlN masks. In [7] it was reported that AlN mask provided very high selectivity to SiO_2 when the gas composition of C_4F_8/SF_6 mixture, pressure and bias power are properly tuned. Similarly, in [8] it was reported that in ICP-RIE system with SF_6/O_2 plasma, the etch rate of AlN can be brought down to 1 nm/min. Though both paper results were obtained only with blanket wafers without any mask pattern, they are a good hint for researches to continue process development in this direction. Also it should be noted that in all cited papers the experiments were performed with wafers of diameter ≤ 150 mm. Now mainstream MEMS industry widely adopts 200 mm substrates but information on deep glass etch on these substrates is scarce so far. Due to complexity of plasma etching, the transfer of a process to wafers of larger diameter rarely reduces simply to scaling of basic process parameters in accordance with scaling of wafer diameter. Besides, sometimes full scaling is not possible due to limitations of RF generators and pumps. In most cases an extensive design of experiment is required. Thus, the purpose of this paper is to investigate possibilities for deep etching of undoped silicon oxide glass (USG) with hard masks on 200 mm substrates in industrial equipment. Since chemical composition of USG, silica and quartz is the same it is feasible to use USG for etching study with a view of potential application of results for etching of silica and quartz.

2. Experimental

We deposited amorphous USG films with thickness up to 21 μm by plasma enhanced chemical vapor deposition (PECVD) on 200 mm silicon wafers in a Sequel Express Concept 2 chamber from Novellus Systems, Inc. using $SiH_4/N_2O/N_2$ gas chemistry. USG etch process development was performed in Omega® advanced planar source (APS) process module from SPTS Technologies which has two high density 13.56 MHz plasma sources (ICP and CCP) , designed to etch materials which are difficult to etch using conventional RIE or ICP sources. The process chamber is of metallic construction and its walls are heated to 130°C to reduce the level of deposition on it, thereby increasing process stability and the mean time between cleans. Through the use of permanent magnets, the plasma is confined, contributing to an increase in plasma density necessary for the successful etching of strongly bonded materials [9]. Wafer is sitting on the cooled chuck with electrostatic clamping and helium backside cooling. The distance from the wafer chuck to the top chamber plate is 225 mm. If otherwise is not stated, the temperature of the chuck was maintained by the chiller at 10 °C.

Two types of hard masks were evaluated in this study. First mask was Al deposited by conventional sputtering. Second mask was AlN deposited by reactive sputtering with pulsed direct current magnetron and RF biased chuck in a Sigma® Deposition System from SPTS Technologies. It should be mentioned that before deposition of AlN the surface of USG was subjected to chemical mechanical polishing to remove USG layer of about 200 nm. This step reduced the surface roughness of USG from 6.2 to 0.2 nm (rms) and enabled high quality of deposited AlN. Patterning of Al mask was performed by standard

lithography and etching with photoresist mask while patterning of AlN was performed with dual mask of photoresist and SiN. The latter was deposited in Sequel Express Concept 2 chamber. Before lithography step, the **s**tress on wafers was minimized by depositing compensating SiN layer on the backside. It allowed to maintain maximal wafer warpage within 50 μm. SiN etching was performed in APS chamber with CF_4/H_2/He chemistry followed by photoresist stripping and wet clean. Etching of Al and AlN was performed with photoresist and SiN masks, respectively, in the same Omega® etch system using ICP-CCP metal etch process module incorporating a radial coil design. A basic gas mixture of Cl_2 /BCl_3 /Ar was used for Al etching while for AlN a buffer gas was added as described in [11]. For both masks the resulting sidewall profile was close to vertical. Tilted scanning electron microscope (SEM) image after AlN hard mask etching is presented in figure 1.

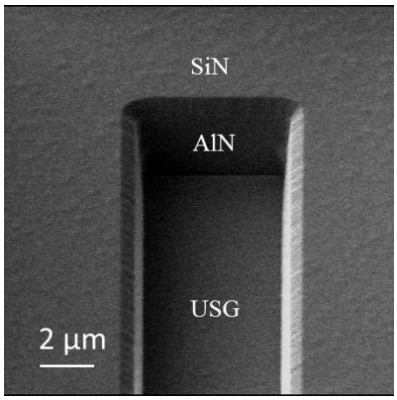

Figure 1. Tilted SEM- image of 2.0 μm-thick AlN mask with top remaining SiN layer after etching in Omega® ICP-CCP process module.

Remaining SiN on top of AlN was not removed and served as an additional mask during short initial period of USG etching. Remaining photoresist mask on Al was removed before USG etch. For both Al and AlN masks, the wafers were subjected to wet clean for metal etch by-products removal before USG etch.

3. Results and discussion

3.1 Aluminum mask

Initial recipe for 150 mm wafers reported in [10] had the following set of parameters: coil (ICP) power 1800 W, platen (bias) power 150 W, pressure 6 mT, flow rates C_4F_8/O_2= 80/10 sccm, chuck temperature 55° C. To scale this recipe for etching of 200 mm wafers, we would need to ramp up RF powers proportionally to the increase of wafer area i.e. by 1.8 times. Calculation yields required coil power of 3200 W and platen power of 270 W. However, requirement of the increased coil power could not be fully satisfied in our 200 mm APS process module due to limitation of maximal power of the RF generator available at out facility. Thus, we tested the recipe with coil power 2000 W and platen power 300 W (other parameters were taken from the recipe for 150 mm wafers). The outcome of etch process was smooth etched bottom, however, sidewall was tapered with the angle of 83° (figure 2), comparing to angle ≥ 88° reported for 150 mm wafers.

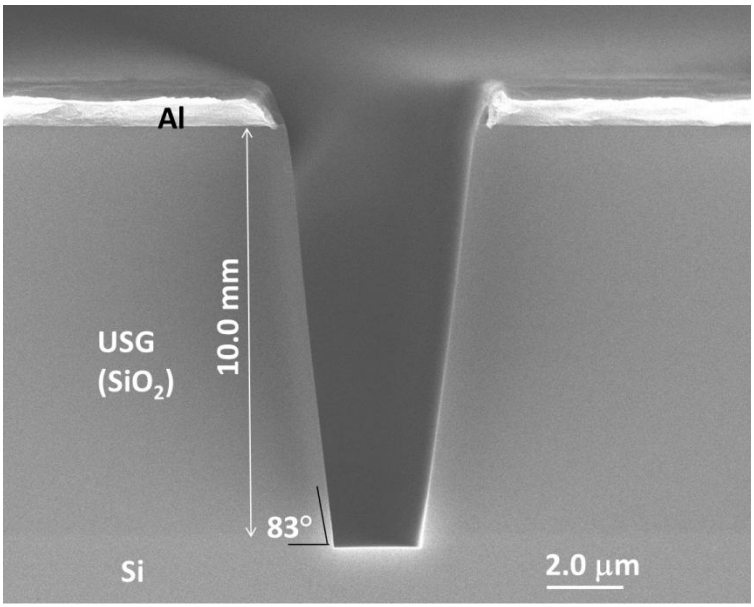

Figure 2. Cross-sectional SEM image of 10 µm-thick USG etched with Al mask using gas chemistry C_4F_8+O_2 (coil/ platen power 2000/300 W, pressure 6 mT , chuck temperature 55°C).

Definitely, the lack of coil power for 200 mm wafers resulted in the non-sufficient ion density. As explained in [13], the result was an increase in passivating neutral-to-ion flux ratio leading to more tapered profile due to increasing re-deposition of C-rich byproducts on sidewalls. Therefore, in order to achieve vertical profile we decided to study effect of reduction of C/F ratio in the gas chemistry by diluting C_4F_8 with CF_4. Figure 3 shows the dependence of USG etch rate and sidewall angle in 5-µm wide trench versus C_4F_8 percentage in the mixture with CF_4. It is seen that the reduction of C_4F_8 percentage resulted in improvement of the sidewall angle even at a lower chuck temperature of 10°C used in these experiments. With full exclusion of C_4F_8, sidewall angle reached the value of 88°. Figure 4 presents cross-sectional image of 4µm- thick USG etched in pure CF_4 plasma.

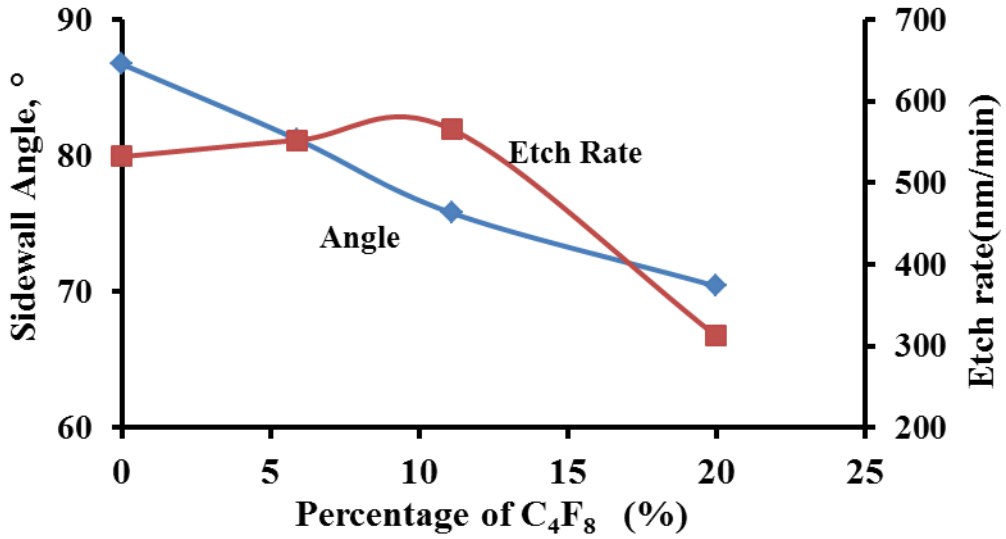

Figure 3. USG etch rate and sidewall angle versus percentage of C_4F_8 in the mixture with 80 sccm of CF_4 (coil/platen power 1600/200 W, pressure 4 mT).

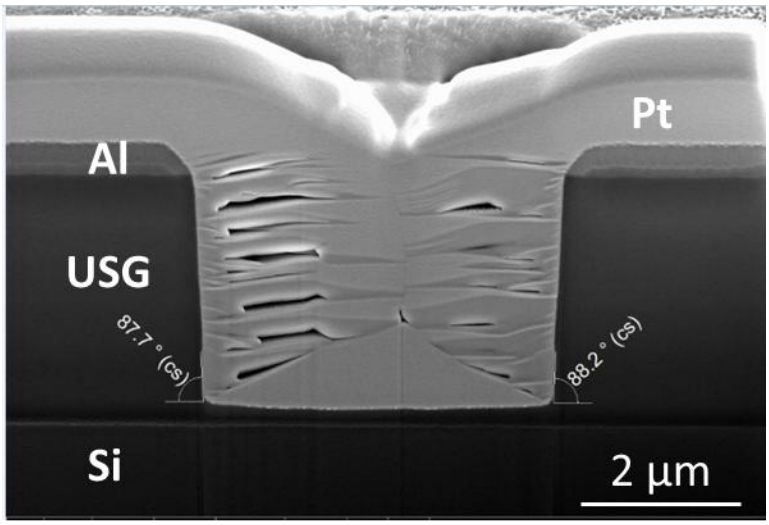

Figure 4. Cross-sectional SEM image of 4 µm-thick USG etched in pure CF_4 with resulting sidewall angle 88° (coil/platen power 1600/200 W, flow rate 80 sccm, pressure 4 mT). Cross-section was done by focused ion beam with preliminary deposition of protective Pt layer.

However, it is also obvious from figure 4 that the facet on Al mask generated by sputtering during USG etch will affect pattern transfer fidelity during deeper etching. Therefore, it is desirable to reduce energy of bombarding ions in order to increase selectivity to mask. Obvious approach in this case is to reduce platen power. However, we found that with the reduction of platen power down to 100 W a phenomenon of micromasking happened in the vicinity of Al mask even in features as large as 18 µm (figure 5).

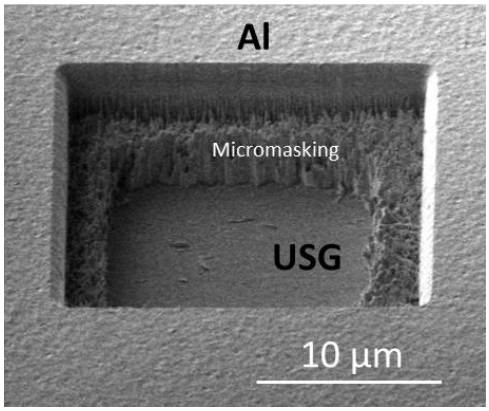

Figure 5. Tilted SEM image of USG etched with Al mask using CF_4 chemistry at 100 W platen power (coil power 1600 W, flow rate 80 sccm, pressure 4 mT).

The cause of micromasking is sputtering and re-deposition of Al mask as confirmed by the presence of strong Al peak in EDX spectrum of micromasked area. Further experiments proved that with pure

CF_4 chemistry, the minimal platen power allowing reliably to avoid micromasking in features of ≥ 5.0μm was 150 W. Therefore, this value of platen power was chosen for evaluation of high aspect ratio etching. Figure 6 presents results of etching of 10 μm-thick USG using Al mask and CF_4 chemistry. An average etch rate in 5 μm-wide trench was 0.39 μm/min, selectivity USG/Al was17:1.

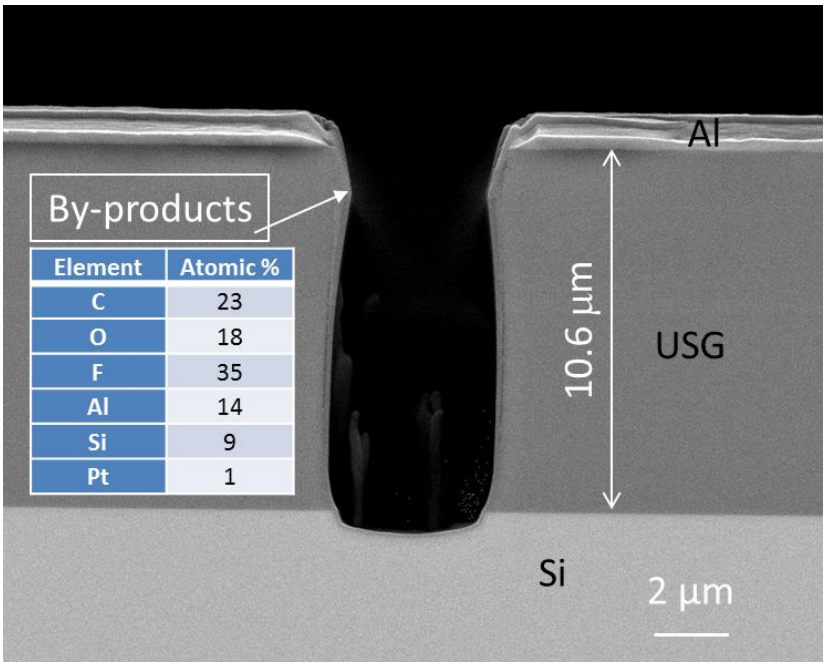

Figure 6. Cross-sectional SEM image of 5.0 μm-wide trench etched with Al mask in 10 μm- thick USG using CF_4 chemistry (coil/platen power: 1800/150 W; flow rate 100 sccm; pressure 5mT). Inset: EDX spectrum of by-products re-deposited on sidewall.

It is seen that sidewall profile at the top part of the trench became tapered due to formation of a facet on Al mask and its subsequent transfer into USG layer. Besides, there is visible necking below the top facet due to by-product re-deposition on the sidewall. Though initial Al mask of 2.0 μm was not fully consumed, deeper etching using the same mask thickness and etch recipe was not feasible due to expected bigger tapering of profile and critical dimensions (CD) loss at a trench top. From the inset in figure 6, we see that Al is a substantial part of the sidewall by-products. Thus, for feasibility of deep etching it is imperative to increase selectivity of USG etch to Al mask on the top corner of the pattern i.e. to reduce sputtering effect. However, as mentioned earlier, the possibility of reduction of platen power was already exhausted by reducing it to 150 W. Therefore, we explored another option for increasing selectivity of etching based on the idea of papers [5, 6] where authors converted Al mask into Al_2O_3 by introducing oxidation steps. However, instead of using alternating etch–oxidize steps we presumed that adding O_2 into gas mixture will create competing process of oxidation on Al surface and, thus, decrease the sputtering of Al mask. Hence, selectivity to Al mask was expected to increase. Indeed, selectivity to Al increased with the same bias power of 150 W from 17:1 in pure CF_4 to 23:1 with added 20 sccm O_2. However, this improvement was not sufficient. To understand why approach with added oxygen was not so effective is possible based on the information in [10] where it was reported that adding O_2 to C_4F_8 increased the angular etching yield of SiO_2 by shifting

conditions from net deposition to net etching. Similarly, we explained an increased faceting of Al mask with added O_2 in our case: adding O_2 resulted in the depletion of adsorbed carbon, and Al surface became more exposed to the attack by sputtering ions. Thus, increased sputtering almost canceled the effect of oxidation in our etching chamber. Moreover, [10] reported that for Pyrex etch with Al mask, an increase in O_2 concentration even resulted in the selectivity drop. Therefore, we concluded that adding O_2 into the gas mixture cannot replace approach with cycles of Al oxidation and etching. However, the latter approach also was rejected because of very low throughput. Obviously, instead of trying to oxidize Al mask in the course of etching, it is better to deposit directly the mask of Al_2O_3 or other material providing higher selectivity.

3.2 Aluminum nitride mask

Paper [8] reported, based on blanket wafer study, that both Al_2O_3 and AlN had very high etch selectivity to USG. This is expected because bond dissociation energies for Al-O (502 kJ/mol) and for Al-N (368 kJ/mol) are noticeably higher than for Al-Al (264 kJ/mol) [14]. Therefore, we continued our development using AlN hard mask deposited by reactive sputtering. Initial testing on blanket AlN wafers revealed that with the same CF_4 etching recipe as in figure 6, the selectivity of USG/AlN reached the value of 28:1 comparing to 17:1 for USG/Al. Etching of patterned wafers using AlN mask gave smooth etched bottom. Figure 7 shows that 16.5 μm-deep USG etch was accomplished with 2.0 μm- thick AlN mask, however, the sidewall shows the same two distortions as in the case of Al mask: one is a facet at the top portion of the sidewall and another is a sidewall necking, right below the facet.

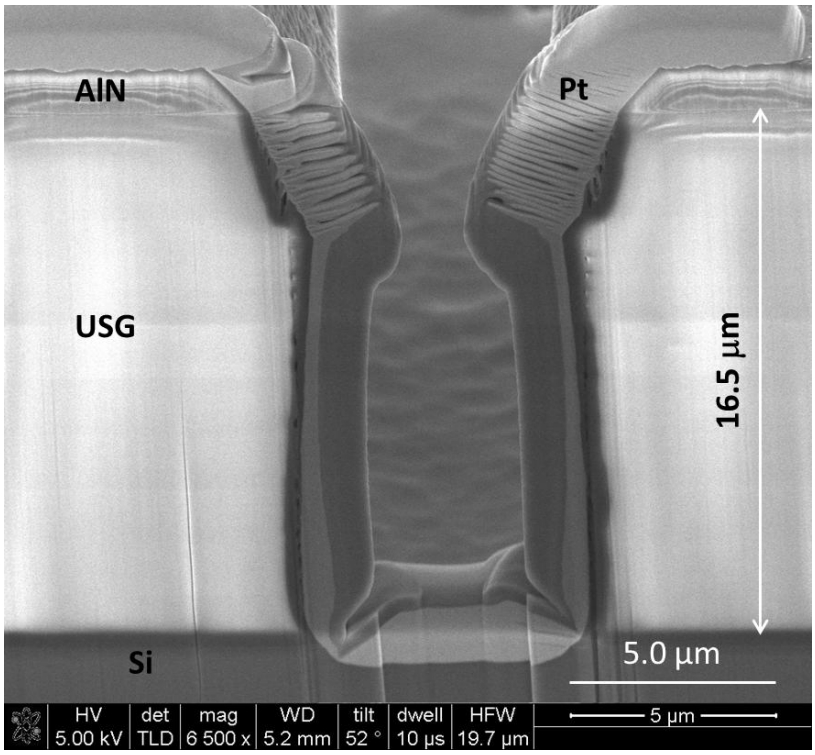

Figure 7. Cross-sectional SEM image of 16.5 μm-thick USG etched with AlN mask using CF_4 plasma (coil/platen power: 1800/150 W; flow rate 80 sccm; pressure 5mT). Pt layer was deposited for protection of the structure during specimen cutting by focused ion beam.

Thus, comparing to Al mask, AlN mask provided fabrication of higher aspect ratio structures in SiO_2, due to higher selectivity, however, additional process tuning was required to overcome issues of corner sputtering and sidewall necking. We presumed that an increase of selectivity would be useful to suppress both mentioned distortions of sidewall profile. Indeed, with an increase of overall selectivity we could expect an increase of selectivity at a top corner as well. At the same time, an increase of selectivity would result in less mask material sputtered and accordingly less material re-deposited on sidewall, thus, decreasing necking. To achieve a decreased necking it seemed reasonable to reduce carbon content in the gas chemistry because we saw high carbon content of 23.4% in the composition of by-products on the sidewall (figure 6). A study of effect of carbon content reduction was implemented by adding SF_6 into gas chemistry and reducing accordingly the fraction of CF_4. Results for the etch rate and selectivity versus percentage of SF_6 in the mixture with CF_4 for blanket wafers are presented in figure 8.

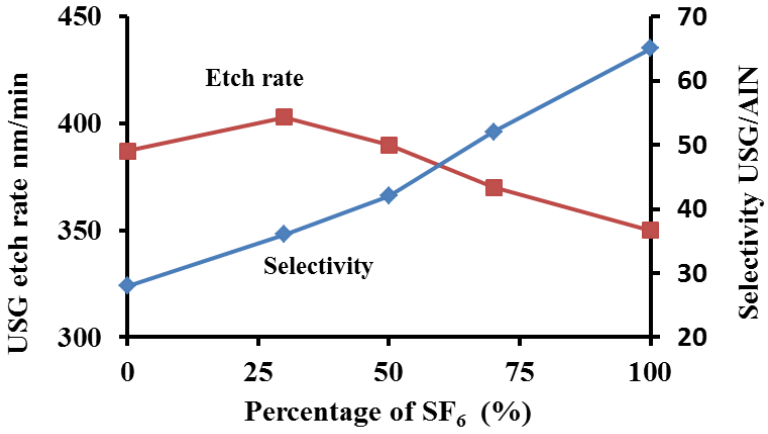

Figure 8. Etch rate and selectivity for blanket wafers versus SF_6 percentage in the mixture SF_6/CF_4 (coil/platen power: 1850/150 W; total flow rate 100 sccm; pressure 5 mT).

It is seen that with the change from 100% CF_4 to 100% SF_6 the selectivity increased almost two-fold though the etch rate of USG somewhat dropped. To compare effects of CF_4 and SF_6 plasma on the sidewall re-deposition we used simplified approach of etching 4 μm-thick USG layer with AlN mask and comparing etch CD bias in 2 μm-wide trenches. It was found that for CF_4 plasma, the trench width after etching shrank by 0.63 μm while for SF_6 plasma only by 0.17 μm. Thus, comparing to CF_4, the SF_6 process provided both better selectivity to AlN mask and less by-product re-deposition on sidewalls. Therefore, we continued SF_6 plasma process optimization. Figure 9 presents USG etch rate and selectivity versus platen power using SF_6 plasma.

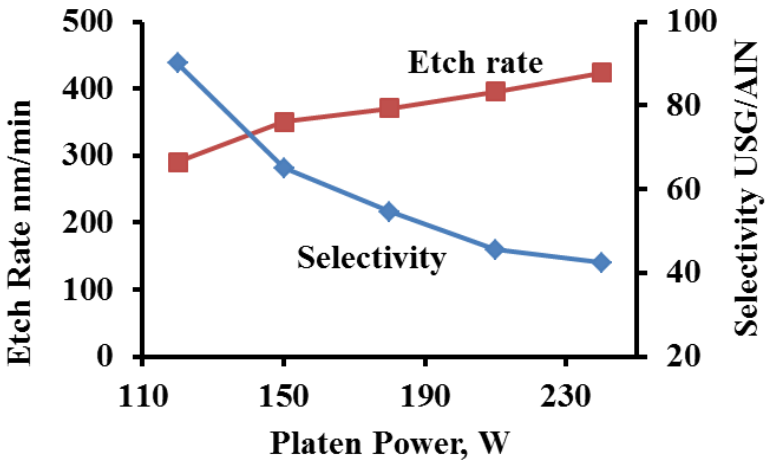

Figure 9. USG etch rate and selectivity for blanket wafers versus platen power in SF_6 plasma (coil power 1850 W, gas flow rate 100 sccm; pressure 5 mT).

It is seen that selectivity drastically improved with the decrease of platen power, however, the etch rate dropped. Similarly to CF_4 etching, there was minimal threshold chuck power of 160 W required to provide micromasking-free etching. To strike a balance between selectivity, etch rate and prevention of micromasking the platen power of 180 W was chosen for etching of patterned wafers. First, we performed partial etching of wafer having trenches of different width and, using cross-sectional SEM images, gathered information on the pattern width dependence of the etch rate (figure 10).

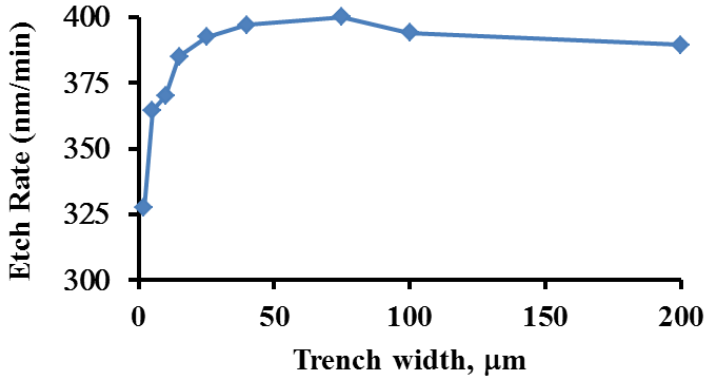

Figure 10. USG etch rate versus trench width for SF_6 plasma etching with AlN mask (coil/platen power: 1850/180 W; flow rate 100 sccm; pressure 5 mT).

From figure 10 it follows that with the increase of trench width from 2 to 25 μm the etch rate increased by 20% and then saturated until trench width reached 75μm. With subsequent increase of the trench width, the etch rate slightly dropped as a result of microloading effect. Also we observed a drop of the average etch rates in trenches with an increased etch depth. For 5μm-wide trenches this drop comprised 16% with the increase of etch depth from 3 to 20μm. This information was used for deciding etch times for full opening of targeted trenches in 21 μm-thick USG on silicon. Figure 11 presents cross-section of 5 μm-wide trench etched by optimized SF_6 recipe.

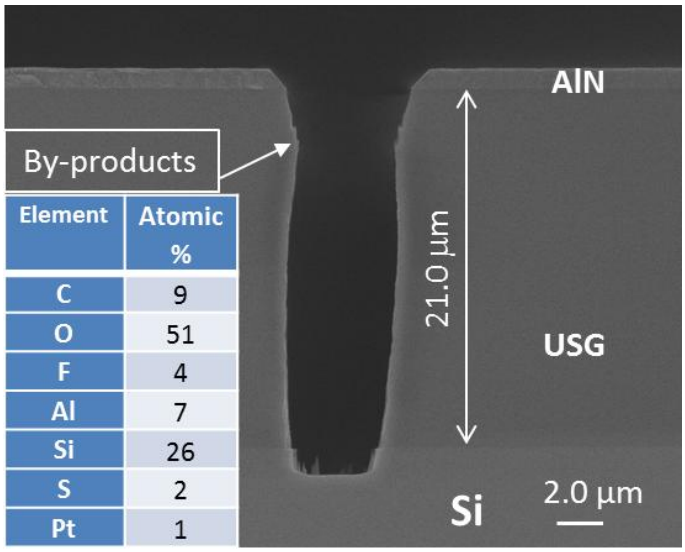

Figure 11. Cross-sectional SEM image of 21 µm-thick USG etched in SF_6 plasma with AlN mask (flow rate 100 sccm, coil/platen power 1850/180 W, pressure 5 mT). Inset: EDX spectrum of by-products re-deposited on sidewall.

Comparing to image in figure 6, where etching was done with Al mask using CF_4 plasma, by-products layer on the sidewall in figure 11 is much thinner and re-deposited Al comprises only 7 atomic % comparing to 23% in case of Al mask. Still some faceting and necking effects is visible in this trench with 4:1 aspect ratio. Figure 12 shows tilted view of arrays of 15 µm-wide cavities after etching with optimized recipe in SF_6 plasma.

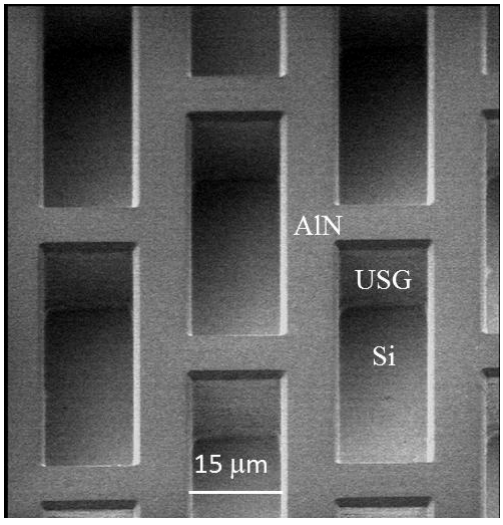

Figure 12. Tilted SEM image of 21 µm- thick USG etched in SF_6 plasma with AlN mask (gas flow rate 100 sccm, coil/platen power 1850/180 W, pressure 5 mT).

It is seen that the sidewall profile of 15-µm wide cavities is close to vertical and etched bottom is smooth. It should be noted that the etch selectivity for patterned wafers is lower than for blanket wafers. We assume that oxygen released during USG etch on patterned wafers helps to remove atoms of sulfur

adsorbed on the surface of AlN mask, thus, making AlN surface exposed to ion bombardment and etching by sputtering. Higher selectivity for patterned wafers was achieved with reduction of platen power from 180 W to 160 W; however, this value of platen power can be used only for trenches with the width of more than 5 μm due to appearance of micromasking on the bottom of narrow trenches at high aspect ratios.

Overall, our study confirmed good prospects of AlN hard mask for deep USG etching because high values of selectivity and possibility to achieve smooth etched bottom have been demonstrated. The results are also applicable to etching of silica and quartz, bearing in mind that, due to higher density of quartz, its etching rate will be slower by 15-20%.

Table 1 presents summary of the etching processes used in this study.

Table 1. Plasma etching processes for each mask material, etch rate and selectivity for 5 μm-wide trenches, sidewall angle and achieved aspect ratio

Mask	Gas chemistry	Platen power, W	Coil power, W	USG etch rate, μm/min	Selectivity to mask	Profile,°	Aspect ratio
Al	$C_4F_8/0_2$	300	2000	0.52	20:1	83	2:1
Al	CF4	150	1850	0.39	17:1	88	2:1
AlN	CF_4	150	1850	0.39	24:1	88	3:1
AlN	SF_6	180	1850	0.36	38:1	88	4:1
AlN	SF6	160	1850	0.32	49:1	88	2:1

Depending on the targeted application, further process optimization may be required for attaining higher values of etch depth or aspect ratio. Another area of improvement is enhancement of etch rate which can be achieved by more detailed process window study. Judging from the mentioned above values of bond dissociation energies of Al-N and Al-O, further improvement of selectivity and other parameters is expected with replacement of AlN mask by Al_2O_3 mask.

4. Summary

We performed optimization of deep etching with hard masks for undoped silicon oxide on 200 mm wafers. Comparing to Al mask, AlN mask enabled higher selectivity and etching profile closer to vertical. Out of three studied gas chemistries - C_4F_8/O_2, CF_4 and SF_6, the latter provided the least amount of by-products re-deposited on sidewalls and, hence, is most suitable for high aspect ratio etching. Optimized etching process with SF_6 plasma yielded structures of 4:1 aspect ratio in 21μm-thick USG. AlN mask is easier to manufacture comparing to such masks as Ni and Cr, which require complicated processes of electroplating and lift-off. Thick AlN mask (up to 3 μm) can be prepared by standard processes of reactive sputtering, lithography and plasma etching. Based on confirmed selectivity values we expect that masking and etching capability developed in this work is extendable for etching of silica and quartz to the depth around 100 μm.

Acknowledgements

The authors would like to thank Dr. Navab Singh from MEMS department of Institute of Microelectronics (A*STAR) for his valuable comments.

References:

[1] Chambers A. 2005 Selectivity/etch rate trade-offs in deep and high A/R oxide etching *Solid State Technology*, issue 2

[2] Ichiki T, Sugiyama Y, Ujiie T, and Horiike Y 2003 Deep dry etching of borosilicate glass using fluorine-based high-density plasmas for microelectromechanical system fabrication *J. Vac. Sci. Technol. B* **21** (5) 2188-2192

[3] Kolari K, Saarela V and Franssila S 2008 Deep plasma etching of glass for fluidic devices with different mask materials *J. Micromech. Microeng.* **18** 064010 (6pp)

[4] Minnick M D, Devenyi G A and Kleiman R N 2013 Optimum reactive ion etching of *x*-cut quartz using SF_6 and Ar *J. Micromech. Microeng.* **23** 117002 (6pp)

[5] Li W T, Bulla D A P, Love J and Luther-Davies B 2005 Deep dry-etch of silica in a helicon plasma etcher for optical waveguide fabrication *J. Vac. Sci. Technol. A* **23(1)** 146–150

[6] Li W-T, Bulla D A P, Boswell R 2007 Surface oxidation of Al masks for deep dry-etch of silica optical waveguides *Surface & Coatings Technology* **201** 4979–4983

[7] Kolari K 2008 High etch selectivity for plasma etching SiO_2 with AlN and Al_2O_3 masks *Microelectronic Engineering* **85** 985–987

[8] Perros A, Bosund M, Sajavaara T, Laitinen M, Sainiemi L, Huhtio T, and Lipsanen H 2012 Plasma etch characteristics of aluminum nitride mask layers grown by low-temperature plasma enhanced atomic layer deposition in SF_6 based plasmas *J. Vac. Sci. Technol. A* **30** (1), Jan/Feb pp 011504-1 - 011504-5

[9] http://www.spts.com/products/plasma-etch/aps-dielectric-etch

[10] Gardner G and Sheldon B 2007 STS Advanced Oxide Etch DRIE System Trends *https://www.bioinformatics.purdue.edu/discoverypark/nanotechnology/facilities/manuals/STS_AOE_DRIE_Trends.pdf*

[11] Bliznetsov V, Johari B H, Chentir M T, Li W H, Wong LY, Merugu S, Zhang X L and Singh N 2013 Improving aluminum nitride plasma etch process for MEMS applications *J. Micromech. Microeng.* **23** 117001 (6pp)

[12] Yin Y and Sawin H H 2008 Angular etching yields of polysilicon and dielectric materials in Cl2/Ar and fluorocarbon plasmas *J. Vac. Sci. Technol. A* **26** (1), 161-173

[13] La Magna A and Garozzo G 2003 Factors Affecting Profile Evolution in Plasma Etching of SiO_2 Modeling and Experimental Verification *Journal of The Electrochemical Society*, **150 (**10) F178-F185

[14] Luo, Y. R., 2007 *Comprehensive Handbook of Chemical Bond Energies*, CRC Press, Boca Raton, FL